JCB Article

ADF/cofilin use an intrinsic mode of F-actin instability to disrupt actin filaments

Vitold E. Galkin,[1] Albina Orlova,[1] Margaret S. VanLoock,[1] Alexander Shvetsov,[2] Emil Reisler,[2] and Edward H. Egelman[1]

[1]Department of Biochemistry and Molecular Genetics University of Virginia Health Sciences Center, Charlottesville, VA 22908
[2]Department of Chemistry and Biochemistry and the Molecular Biology Institute, University of California, Los Angeles, CA 90095

Proteins in the ADF/cofilin (AC) family are essential for rapid rearrangements of cellular actin structures. They have been shown to be active in both the severing and depolymerization of actin filaments in vitro, but the detailed mechanism of action is not known. Under in vitro conditions, subunits in the actin filament can treadmill; with the hydrolysis of ATP driving the addition of subunits at one end of the filament and loss of subunits from the opposite end. We have used electron microscopy and image analysis to show that AC molecules effectively disrupt one of the longitudinal contacts between protomers within one helical strand of F-actin. We show that in the absence of any AC proteins, this same longitudinal contact between actin protomers is disrupted at the depolymerizing (pointed) end of actin filaments but is prominent at the polymerizing (barbed) end. We suggest that AC proteins use an intrinsic mechanism of F-actin's internal instability to depolymerize/sever actin filaments in the cell.

Introduction

Actin-depolymerizing factor (ADF)/cofilin (AC) proteins are ubiquitous in eukaryotic organisms. Because these proteins have been given many different names (destrin, depactin, etc.) we will collectively refer to them as AC proteins. They are responsible for the rapid rearrangement of actin structures in the cell (Bamburg, 1999), and these proteins have been shown to play a crucial role in cell motility (Carlier and Pantaloni, 1997), cell division (Abe et al., 1996), and endocytosis (Lappalainen and Drubin, 1997). AC proteins bind to monomeric G-actin and can bind to filamentous F-actin in a 1:1 (Bamburg, 1999) and 2:1 (Galkin et al., 2001) stoichiometry. All AC proteins that have been characterized in vitro disrupt actin more readily at higher pH (Yonezawa et al., 1985) except for *Acanthamoeba* actophorin (Maciver et al., 1998) and starfish depactin (Bamburg, 1999). One mechanism for a pH dependence of F-actin depolymerization has recently been proposed and involves a gain of nucleating activity for the ADF–actin complex at low pH (Yeoh et al., 2002).

Filament severing was originally suggested to be the main mechanism of depolymerization of actin filaments by AC proteins (Cooper et al., 1986; Maciver et al., 1991), but it was subsequently argued that F-actin depolymerization occurs through an acceleration of treadmilling (Carlier, 1998). Further experiments revealed that both mechanisms exist in the activity of AC proteins. The binding of AC proteins to G-actin has been separated from the binding to F-actin by site-specific mutagenesis, and a severing activity was separated from a depolymerizing one (Pope et al., 2000; Ono et al., 2001).

It was suggested that the change in twist observed upon binding of AC to F-actin (from ~167° per subunit in undecorated filaments to ~162° per subunit in F-actin complexed with AC) and a proposed weakening of the longitudinal contacts in F-actin were responsible for the destabilization of the actin filament (McGough et al., 1997). It was subsequently found that a mutant AC protein could change the twist of F-actin without depolymerization (Pope et al., 2000), suggesting that the change of twist alone was not sufficient for depolymerization. It was also shown that significant amounts of actin segments having a twist of 162° and smaller could be found in the absence of any AC proteins within pure F-actin filaments, leading to the notion that AC proteins are stabilizing an intrinsic

Address correspondence to Edward H. Egelman, Department of Biochemistry and Molecular Genetics, University of Virginia Health Sciences Center, Jordan Hall, Charlottesville, VA 22908-0733. Tel.: (434) 924-8210. Fax: (434) 924-5069. email: egelman@virginia.edu

Key words: actin; electron microscopy; cytoskeleton

Abbreviations used in this paper: AC, ADF/cofilin; ADF, actin-depolymerizing factor; IHRSR, iterative helical real space reconstruction; pADF, plant ADF; SD1, subdomain 1; y-cofilin, yeast cofilin.

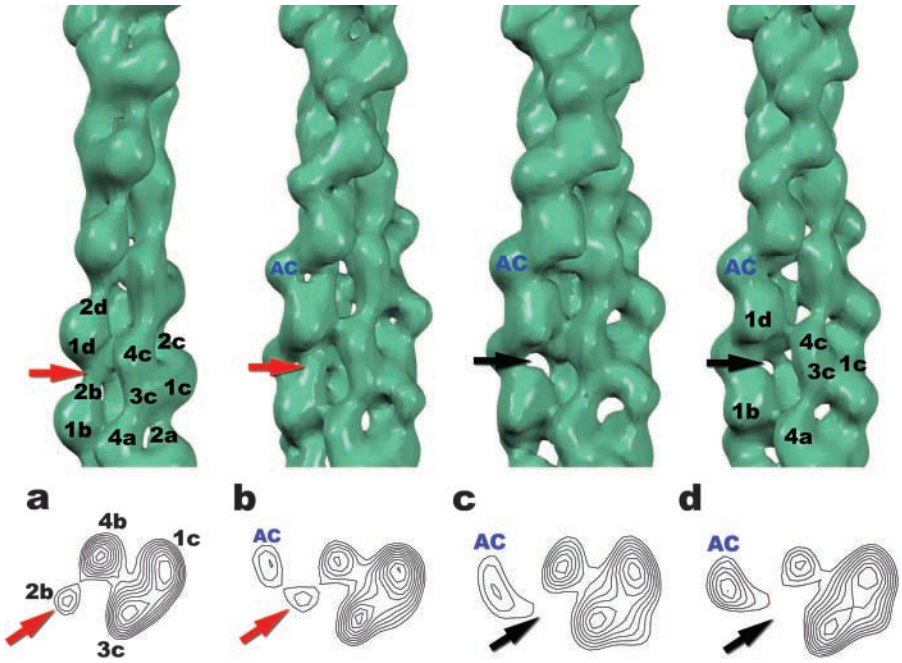

Figure 1. **Disruption of SD2–SD1 contact is a function of occupancy.** Three-dimensional reconstructions of pure F-actin (a), pADF-F-actin complex, pH 6.5 (b and c), and pADF-F-actin complex, pH 7.7 (d). Surfaces are shown at the top, while cross sections of the respective reconstructions are shown at the bottom. The four actin subdomains are labeled 1–4, and four successive protomers are indicated as a–d. The additional mass due to the AC protein bound at the primary site is indicated by the AC labels in b–d. The averaged pH 6.5 complex (b) has been found to contain a variable amount of bound pADF. A subset corresponding to nearly saturated binding (c) looks very similar to the pH 7.7 complex (d) that was much more homogeneous with respect to pADF binding, showing that the differences between b and d can mainly be explained by different amounts of pADF bound. It can be seen in the cross sections that more pADF is bound in the averaged pH 7.7 reconstruction (d) than in the high occupancy pH 6.5 reconstruction (c). The red arrows (a and b) mark the density of SD2, which forms a link with SD1 of the protomer above on the same long-pitch helical strand. This link is still present in b when there is a partial occupancy by pADF, but the density is attenuated in comparison with that present in pure F-actin (a). With greater occupancy at pH 6.5 (c) or at pH 7.7 (d), this link is absent (black arrow, c and d).

conformation of F-actin, rather than inducing a novel state of twist (Galkin et al., 2001).

Based on EM observations, the disruption of lateral contacts (between the two strands of F-actin) was also proposed to be part of the AC depolymerization mechanism (McGough and Chiu, 1999). The finding of an additional AC binding site on the "back side" of subdomain 1 (SD1; the opposite surface from that originally shown to be the site of AC binding; McGough et al., 1997) led to a different suggestion for F-actin disruption by AC molecules: that cofilin mechanically disrupts actin filament by intercalation between two adjacent actin protomers within one helical strand (Blondin et al., 2001). It was shown that at high pH, this second site is occupied by a second AC molecule (Galkin et al., 2001). All of these observations suggest that the structural complexity of the interactions of AC proteins with actin is still poorly understood. Part of this complexity may have to do with the structural polymorphism of F-actin (Egelman, 2003a).

A remarkable feature of actin, widely used by motile cells, is its ability for fast polymerization/depolymerization through reversible, noncovalent association of G-actin into filaments. After polymerization, F-actin is still a dynamic system when ATP is present in vitro. Due to the difference in affinity of ATP- and ADP-containing monomers for F-actin, filaments slowly lose protomers containing ADP from their depolymerizing (pointed) ends, and monomers containing ATP bind to the growing (barbed) ends. This process, called treadmilling (because it allows a flux of subunits to travel through a filament that is maintained at a steady-state length), is accelerated by AC proteins. The dynamics of actin filament ends is not simply a function of the actin concentration, but can depend upon pH (Sampath and Pollard, 1991) and the cation bound to actin's high affinity metal-binding site (Coluccio and Tilney, 1983). The structural aspects of actin polymerization/depolymerization, involving the conformational changes between the G-actin monomer and the F-actin protomer, and its acceleration by AC proteins are still unknown.

To isolate separate states within AC–F-actin complexes, we have used a single-particle approach to image analysis of helical polymers (Egelman, 2000) that allows three-dimensional reconstruction without needing to average together long stretches of filaments. The ability to analyze thousands of short segments has allowed us to isolate barbed and pointed ends of actin filaments and reconstruct these ends separately. In addition, we have taken advantage of a disulfide cross-link between Cys41 (engineered into a mutant yeast actin) and Cys374 in a neighboring protomer (Kim et al., 2000) to investigate AC–F-actin complexes within filaments that cannot be depolymerized due to the covalent attachments between subunits.

We show that transitions in the DNase I–binding loop are caused by the binding of AC proteins to F-actin, and that these changes lead to the disruption of one of the longitudinal contacts within the actin filament. We show that these changes occur stoichiometrically, in contrast to highly cooperative twist changes induced by AC proteins that can occur substoichiometrically. We demonstrate that the same disordering of the DNase I–binding loop observed in the center of actin filaments complexed with AC proteins also occurs at the pointed ends of pure F-actin. This leads us to suggest that AC proteins use the intrinsic instability of F-actin pointed ends as a part of the mechanism for extensive and rapid depolymerization of actin filaments.

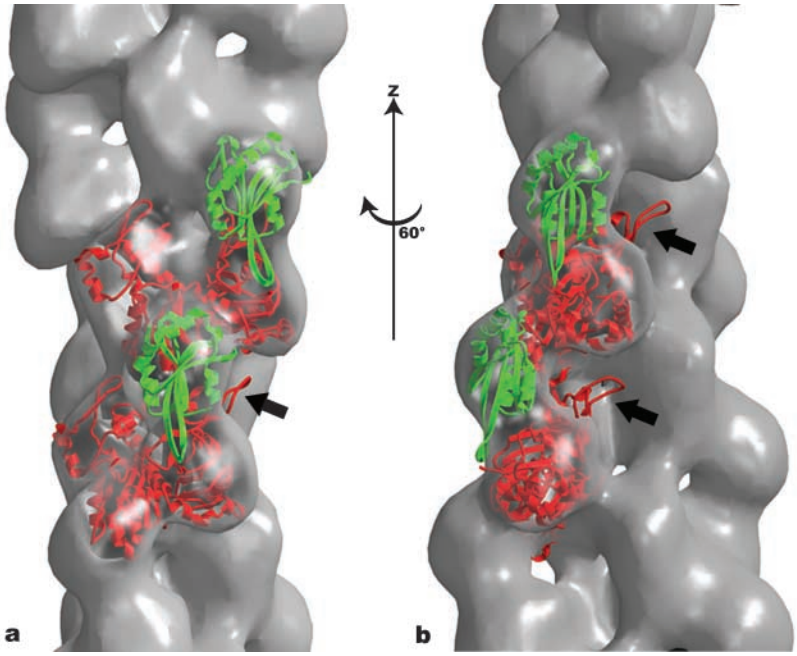

Figure 2. **A molecular model for the actin–pADF complex of Fig. 1 c.** The reconstruction is shown as a semi-transparent gray surface, the crystal structure of an actin monomer (Chik et al., 1996) is drawn in red, and a crystal structure of pADF (Bowman et al., 2000) is in green. Two views of this complex are shown, related by a 60° rotation about the filament axis. The black arrows indicate SD2 of the actin crystal structure. There is no corresponding density for this subdomain in the EM reconstruction, suggesting that it must be largely disordered.

Results

p-ADF disrupts the contact between SD2 and SD1 in a stoichiometric manner

It was previously shown that at pH 6.5, plant ADF (pADF) bound to muscle F-actin predominantly at a 1:1 stoichiometry (Galkin et al., 2001). At a higher pH (7.7), partial binding of a second pADF molecule to each actin protomer was observed, but only traces of this second molecule could be visualized. Thus, the pADF–actin complex is a good system for looking at the details of interaction of the primary AC molecule with F-actin, without the additional complexity introduced by the extensive binding of the second AC molecule.

At pH 6.5 (Fig. 1 b), the additional mass due to the pADF molecule bound at the primary site was less than that observed at pH 7.7 (Fig. 1 d). This can be seen more clearly in a comparison of the cross sections than of the surfaces. At pH 6.5, only ~11% of segments were classified as having occupancy close to 100%, while at pH 7.7, ~92% of the segments were classified as having maximal occupancy. Using the projected densities (see Materials and methods), we were therefore able to separate the filament segments at pH 6.5 into three classes, based upon the extent of occupancy: low, intermediate, and high. The high occupancy reconstruction is shown in Fig. 1 c. The intermediate class (not depicted) was almost indistinguishable from the average (Fig. 1 b), as we would expect for an average that contains a range of occupancies. In contrast, the average at pH 7.7 (Fig. 1 d) could not be decomposed into sets showing different amounts of binding by pADF, suggesting that it was much more homogeneous. All sets, however, showed a twist of ~162° per actin protomer, indicating that there was ~5° change per protomer induced by the pADF molecules. This twist change was independent of the extent of binding. In fact, the difference in twist of the low and high occupancy sets was within experimental error (<0.3°). This shows that the twist change must be cooperative, and propagated to adjacent actin protomers that do not have a pADF molecule bound.

Another difference among the reconstructions shown in Fig. 1 is a change in F-actin structure. Tests for the significance of these differences (see Materials and methods) suggest that they are highly reproducible. In a control F-actin reconstruction, SD2 makes a strong contact with SD1 of the protomer above in the same long-pitch helical strand (Fig. 1 a, red arrows). In the averaged reconstruction of pADF at pH 6.5, this contact is attenuated, but still remains prominent (Fig. 1 b, red arrows). At pH 7.7, this contact no longer exists (Fig. 1 d, black arrow). We can exclude the possibility that these changes in F-actin, including the loss of the SD2–SD1 contact, are due to a pH effect on F-actin, as control reconstructions of F-actin alone at these two pH values did not show this structural change (unpublished data). By reconstructing the ~11% of segments classified as having maximal occupancy at pH 6.5 (Fig. 1 c), we found that the contact between SD2 and SD1 of the adjacent protomers in the same strand is absent. Thus, it appears that the pH-dependent difference in this contact (Fig. 1, b and d) is predominantly due to the difference in the amount of pADF bound to F-actin. In contrast to the change in twist, which occurs completely at substoichiometric binding of pADF, the change in the SD2–SD1 contact appears to be proportional to the amount of pADF bound to F-actin. A possibility that needs to be considered is that the lower perceived occupancy by pADF in certain three-dimensional reconstructions is actually due to greater disorder in these classes, and not lower occupancy. We can exclude this possibility because the sorting into classes was based upon projected density within a certain radial region. If the pADF molecules were bound, but disordered, they would still contribute to the projected density. We therefore think that the smaller mass seen for the pADF in certain classes truly represents lower occupancy.

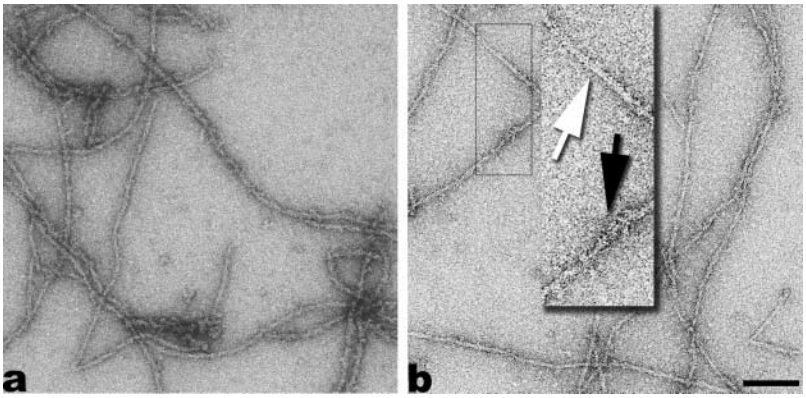

Figure 3. **Electron micrographs of wild-type yeast actin and disulfide cross-linked yeast actin after incubations with y-cofilin.** Wild-type actin filaments (a) are uniformly decorated by y-cofilin, while the decoration of cross-linked actin filaments (b) is variable. In b, one region (boxed) is magnified in the inset. The black arrow indicates a region of heavy decoration, while the white arrow indicates a section that appears to be mainly naked F-actin. Bar, 1,000 Å.

The observed reconstructions suggest two likely possibilities for how the pADF bound to F-actin could eliminate the SD2–SD1 contact. One is that SD2 of actin could be significantly shifted in position, the other is that SD2 could become extensively disordered and thus not be visualized. Both possibilities are consistent with a large body of experimental data. For example, significant SD2 shifts in G-actin have been observed crystallographically (Chik et al., 1996; Otterbein et al., 2001), and EM reconstructions have been interpreted as showing SD2 shifts within F-actin (Owen and DeRosier, 1993; Orlova and Egelman, 1993; Belmont et al., 1999). On the other hand, a portion of SD2 (the DNase I–binding loop) was not observed in one crystal structure due to disorder in this region (McLaughlin et al., 1993), and other F-actin reconstructions have been interpreted as missing part or all of the density due to SD2 (Bremer et al., 1994; Orlova et al., 1995). We have therefore used atomic models (Fig. 2) in an attempt to distinguish between these possibilities. If SD2 was shifted, then density from this region would be appearing elsewhere. Given that SD1, -3, and -4 are fit well in the reconstruction by an atomic model of the actin monomer, with the nucleotide-binding cleft in the "open" state (Chik et al., 1996), the only place this density might appear if it was shifted would be in the density attributed to pADF. However, this density is also fit well by an atomic structure for pADF (Bowman et al., 2000). The possibility that the occupancy of this site by pADF is <100%, and that some of this density is due to SD2, is unlikely, as this would lead to more density at the bottom of this region, which is not seen. We are left with the possibility that SD2 is likely to be extensively disordered. Further evidence in support of this possibility arises from other studies (see next two sections).

Cross-linking the DNase I–binding loop to the COOH terminus within F-actin affects the binding of AC molecules

We have shown (previous section) that the contact between DNase I–binding loop (within SD2) and the COOH terminus (within SD1) of an adjacent protomer is strongly affected by the binding of pADF. To examine this in more detail, we have used a mutant yeast F-actin where Gln41 is substituted with a cysteine (Kim et al., 2000). Under oxidizing conditions, this mutation allows for disulfide cross-link formation between SD2 (Cys41) of one protomer and SD1 (Cys374) of an adjacent protomer in the same long-pitch helix strand. This cross-link introduces very little structural perturbation into F-actin (Orlova et al., 2001) and thus should be useful in studying the interactions with AC and other actin-binding proteins that may introduce larger perturbations into F-actin structure. While Fig. 1 shows the results of studies done with pADF (at pH 6.5 and 7.7), we have used yeast cofilin (y-cofilin) at an intermediate pH (7.2) to examine the interaction with the disulfide cross-linked yeast F-actin.

Fig. 3 shows electron micrographs of complexes of y-cofilin with wild-type yeast F-actin (Fig. 3 a) and cross-linked filaments (Fig. 3 b). Filaments in Fig. 3 a look decorated when compared with pure F-actin filaments. In contrast, two distinct types of filaments are observed when y-cofilin is incubated with disulfide cross-linked actin filaments. Parts of the filaments resemble the wild-type actin complexes (Fig. 3 b, black arrow), but other regions have a smaller diameter (Fig. 3 b, white arrow). Both regions can be found within the same F-actin filament. As a control, all experiments were also done with the Q41C yeast actin mutant (used for the disulfide cross-linked filaments) under reducing conditions. These complexes were indistinguishable from the complexes formed with wild-type yeast actin, suggesting that the differences found with the disulfide cross-linked filaments are not due to the amino acid change at residue 41 in actin.

However, the possibility exists that the difference in binding of y-cofilin to disulfide cross-linked F-actin might be due to modifications of the AC molecules resulting from oxidizing conditions. In the absence of a reducing agent, it has been shown that y-cofilin greatly inhibits the formation of interprotomer disulfides in F-actin, and that this must arise from binding extensively to F-actin (Bobkov et al., 2002). Thus, the oxidizing conditions have been shown to not inhibit the binding of y-cofilin to F-actin. Moreover, y-cofilin has only one cysteine residue, which excludes the possibility of internal disulfides. We were not able to find any significant bundle formation, which might take place if a dimerization of y-cofilin occurred.

Using 28,900 filament segments extracted from the complexes of y-cofilin with both wild-type and disulfide cross-linked F-actin, we sorted images into three classes: pure (undecorated or poorly decorated) F-actin, singly occupied, and doubly occupied. The single (1:1) and double (2:1) occupancy arises from the two sites at which AC molecules can bind to F-actin (Galkin et al., 2001). Because the focus of

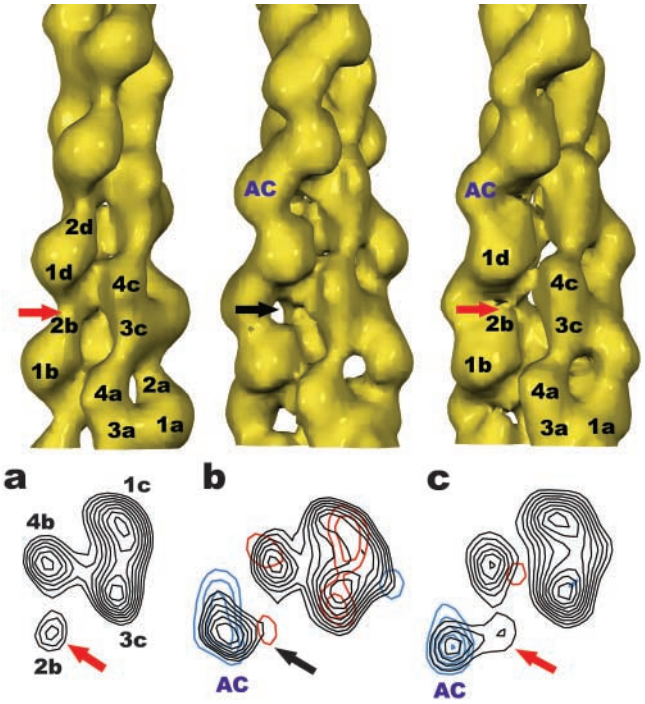

Figure 4. **Comparison between wild-type and cross-linked decorated filaments.** Reconstructions (surfaces, top, and contour plots, bottom) are shown for pure F-actin (a) and filaments singly decorated with y-cofilin (b and c). The decorated filaments are either wild-type yeast F-actin (b) or disulfide cross-linked F-actin (c). The actin subdomains are labeled as in Fig. 1, and the red arrows (a and c) indicate the density of SD2 that is making a link with SD1 of the protomer above. The black arrow (b) indicates where this link is broken as a result of the binding of the AC molecule at the primary site (i.e., between the bottom of 1d and the top of 2b). Because the disulfide cross-link enforces a covalent attachment of SD2 (residue 41) of one protomer to SD1 (residue 374) of a protomer above, this link cannot be broken by the AC binding, and can actually be visualized (red arrow, c). The blue contour lines represent positive differences when the pure F-actin map (a) is subtracted from the occupied volumes (b and c), and these indicate the mass due to y-cofilin. The red contour lines represent the negative differences, and show conformational changes within F-actin. These conformational changes are much greater in wild-type F-actin (b) than they are within disulfide cross-linked F-actin (c) where covalent constraints have been introduced between subunits. The lowest difference contours correspond to $\sim 3\sigma$, based upon estimates of the uncertainty in the reconstructions determined by generating multiple reconstructions from different starting points.

this work was structural changes in F-actin introduced by primary AC molecules, we used segments assigned to the single occupancy class for further analysis.

Reconstruction of complex of y-cofilin with disulfide cross-linked actin

The actual reconstruction of the singly decorated state of y-cofilin with wild-type F-actin (Fig. 4 b) displays no significant differences if compared with pADF–rabbit-F-actin complex at pH 7.8 (Fig. 1 d). Both reconstructions show a significant additional mass (labeled AC in Figs. 1 and 4) that bridges the lower part of SD2 of one actin protomer with the bottom of SD1 of the protomer above it. Both proteins disrupt the contact between SD2 and SD1 of these same protomers (Fig. 4 b, black arrow), as discussed for pADF (Fig. 1). This contact is present in wild-type yeast F-actin (Fig. 4 a, red arrow) as well as in the yeast Q41C mutant actin (not depicted). Introduction of a disulfide cross-link between SD2 and SD1 does not affect the position of the y-cofilin bound to F-actin (Fig. 4 c), but a contact is enforced (by the covalent linkage) between SD2 and SD1 (Fig. 4 c, red arrow). However, this linkage decreases the amount of additional mass bound to actin in comparison with the complex of y-cofilin and wild-type F-actin (Fig. 4 b). Thus, the segments that have been selected as showing single decoration by y-cofilin after disulfide formation in F-actin are actually partially occupied, and are some combination of undecorated and singly decorated actin protomers. This is consistent with the fact that under the same conditions, ~10% of segments are identified as being pure F-actin, while in the absence of the disulfide, all segments are classified as decorated (unpublished data). We can exclude the possibility that the ~10% of segments classified as being pure F-actin are actually the only segments that have been extensively cross-linked by disulfide bonds, because under the conditions that we are using, ~94% of the F-actin subunits are involved in a cross-link with a neighboring subunit (Orlova et al., 2001).

The surfaces of the three-dimensional reconstruction (Fig. 4) are excellent for looking at the geometry of binding of the AC proteins to F-actin, but they are relatively insensitive to internal changes in actin induced by this binding. Cross section shows significant redistribution of mass within SD1 and SD3 of actin protomers when y-cofilin (Fig. 4 b, red contours) is attached to wild-type F-actin. Different conformational changes are present within actin in the disulfide cross-linked actin complexes (Fig. 4 c). While the covalent linkage between SD2 of one protomer and SD1 of another protomer ensures that some contact must exist between these two regions, the extent of this contact is clearly lessened when y-cofilin is bound (Fig. 4 c), consistent with the total loss of this contact in the presence of y-cofilin and the absence of the disulfide in reducing conditions.

Reconstruction of barbed and pointed ends of pure F-actin

We were interested to compare the destabilization of the actin filament induced by AC proteins with the intrinsic instability that can occur at the pointed end of F-actin. After polymerization in the presence of ATP, actin filaments remain dynamic systems, adding monomers from one end (barbed end) and losing them from the opposite one (pointed end). It is therefore interesting to look at the structural state of the two ends to understand the mechanistic basis for why one end is losing subunits and the other end is gaining subunits. Using a single particle approach to helical reconstruction (Egelman, 2000), this comparison is now possible.

After 2 h of polymerization under low-shear conditions, F-actin exists as relatively long filaments with a small number of ends present. We analyzed ~40 electron micrographs to extract ~1,300 filament ends. A potential problem in reconstructing ends arises from the possibility of filament breakage during sample application to the grid. In this event, some ends would actually represent segments in the interior of a filament. To avoid this, we allowed filament

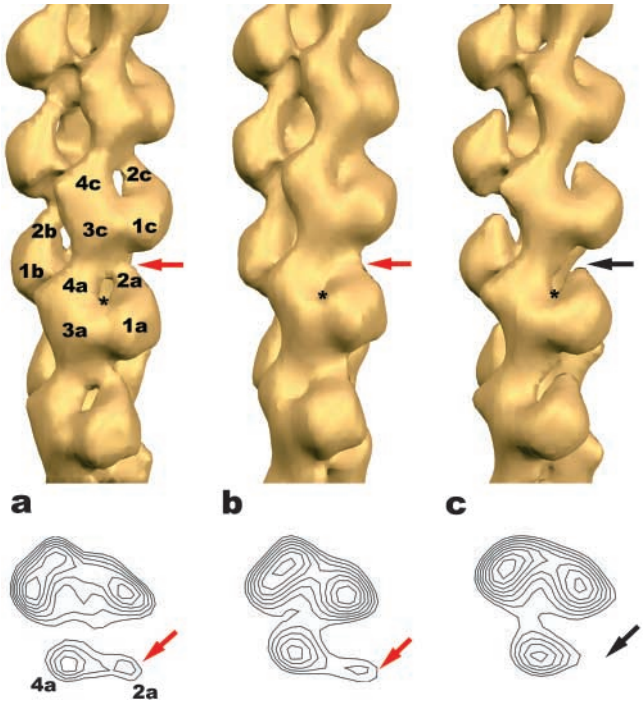

Figure 5. **Comparison of barbed and pointed end reconstructions.** Surfaces (top) and contour plots (bottom) from the three-dimensional reconstructions of control segments from the middle of pure actin filaments (a), from the barbed ends (b), and from the pointed ends (c). The nucleotide-binding cleft (indicated by the asterisks) is open in the center of the filaments (a) and at the pointed end (c), but closed at the barbed end (b). A strong contact exists between SD2 and SD1 above it in the central segments (a, red arrow) and at the barbed end (b, red arrow), but this contact is missing at the pointed end (c, black arrow).

ends to relax to the steady-state condition by incubating the sample on the EM grid for ~2–3 min with 0.2 mM ATP concentrations before fixation by uranyl acetate (Zhao and Craig, 2003a,b).

The reconstructions of barbed ends, pointed ends, and control segments (from the filament interior) are shown in Fig. 5. The control reconstruction, from the filament interior, shows a prominent contact between SD2 and SD1 of adjacent actin protomers (Fig. 5 a, red arrow; compare with Fig. 1 a and Fig. 4 a) and an open nucleotide-binding cleft (marked with asterisk). In contrast, the reconstruction of the fast growing (barbed) end has a closed cleft (Fig. 5 b, asterisk). The ridge of density between SD2 and SD1 (Fig. 5 b, red arrow) is the same as in the control reconstruction. The reconstruction of the pointed end (Fig. 5 c) has two important features. The cleft is open (Fig. 5 c, black asterisk) to the same extent as in the control reconstruction, and there is no contact between SD2 and SD1 of adjacent protomers in the same long-pitch helical strand (Fig. 5 c, black arrow). We have been able to show that the visualization of an open or closed nucleotide-binding cleft is not simply due to an arbitrary choice of contour levels, as atomic structures of G-actin in an open (Chik et al., 1996) or closed (Schutt et al., 1993) state can be used to distinguish between the state of the F-actin protomer in low resolution reconstructions (Belmont et al., 1999; Orlova et al., 2001; Sablin et al., 2002).

Discussion

The main role of AC proteins in the cell appears to be in the destabilization of actin filaments. However, actin's own hydrolysis of ATP also destabilizes the filament. It has been shown that actin's ATPase activity results in a weakening of the SD2–SD1 longitudinal contacts within F-actin that arises from an opening of the nucleotide-binding cleft between the major domains (Belmont et al., 1999). The fitting of G-actin crystal structures to the AC–F-actin complex (Fig. 2) shows that the actin protomer in these complexes has an open nucleotide-binding cleft, expected for the ADP-bound state (Sablin et al., 2002). This is consistent with the fact that AC proteins bind only to ADP-actin (Carlier et al., 1997). It has already been proposed that cofilin could alter the stability of the longitudinal bonds in the actin filament (McGough et al., 1997), but this suggestion was based upon a predicted consequence of the change in twist, rather than a direct observation. A solution study has directly shown that cofilin shifts the SD2–SD1 interface (Bobkov et al., 2002). With improved methods, we have been able to visualize a large consequence of the interaction of an AC molecule with F-actin, which is disruption of the contact between SD2 and SD1. Previously, we showed that within actin filaments extensively decorated with AC proteins, under conditions favoring depolymerization and severing (high pH), segments of naked actin could be found in which the actin subunits were substantially tilted away from their normal orientation in F-actin (Galkin et al., 2001). This tilt required a breaking of the normal SD2–SD1 contacts in F-actin (Galkin et al., 2002). In the present work, we show that the magnitude of the SD2–SD1 disruption depends upon the extent of AC occupancy, and that for pADF molecules, the increasing occupancy correlates directly with increasing pH. We found that in equally occupied segments, the ability of AC proteins to disrupt the contact between SD2 and SD1 remains the same at high and low pHs.

The disruption of the SD2–SD1 interface by the AC proteins leads to a simple prediction: conditions that disrupt this interface should accelerate the binding of AC proteins to F-actin, while conditions that stabilize this interface should inhibit the binding of AC proteins to F-actin. Available data support this prediction. Cleavage of the DNase I–binding loop in F-actin has been shown to largely eliminate the SD2–SD1 interface (Orlova and Egelman, 1995), and ADF has been shown to bind much more rapidly to such cleaved F-actin with no lag time (Ressad et al., 1998). The release of phosphate after ATP hydrolysis in F-actin destabilizes the filament by weakening the SD2–SD1 interface (Belmont et al., 1999; Sablin et al., 2002). In the presence of beryllium fluoride, which has been shown to maintain F-actin in an F-ADP-P_i state (Combeau and Carlier, 1988), ADF neither bound to F-actin nor depolymerized it (Carlier et al., 1997). Similar conclusions about the inhibition of ADF binding to F-actin were reached using P_i to drive F-ADP actin to the F-ADP-P_i state (Maciver et al., 1991; Maciver and Weeds, 1994).

Relation to spectroscopic studies

There is an excellent agreement and complementarity between the results presented here and previous spectroscopic studies of conformational changes in G-actin (Blondin et al.,

2001; Dedova et al., 2002) and F-actin (Bobkov et al., 2002) induced by the binding of cofilin. In both studies, shifts were seen in actin between SD2 (the DNase I–binding loop) and SD1 (the COOH terminus) induced by the binding of cofilin. While we showed that the binding of AC molecules to disulfide cross-linked F-actin filaments is partially inhibited in comparison to the binding to normal F-actin, Bobkov et al. (2002) showed that if cofilin was first bound to F-actin, the formation of interprotomer disulfides was greatly inhibited. Both experiments show that cofilin binding to F-actin changes the conformation of SD1 and SD2. These experiments offer different insights, however. When an AC molecule is bound first, the result of Bobkov et al. (2002) shows that Cys374 and Cys41 from another protomer are shifted away from each other, greatly suppressing the rate at which disulfide bonds can be formed. The introduction of such covalent cross-links in F-actin can be a powerful tool for looking at the interaction of actin-binding proteins with F-actin.

We have observed a dependence of the disruption of the SD2–SD1 linkage upon the occupancy of pADF at pH 6.5 (Fig. 1), while within these same filaments, we observe a cooperative change in twist that is independent of the extent of binding. Bobkov et al. (2002) showed a number of spectral changes in F-actin that could be monitored as a function of cofilin binding, and these changes were directly proportional to the extent of binding, showing no significant cooperativity. Using different spectroscopic probes, cooperative effects can be seen as a result of cofilin binding to F-actin (Bobkov, A.A., personal communication). Thus, within the same system (complexes of F-actin with AC proteins), some changes in F-actin may occur cooperatively, while other changes may be fairly noncooperative. This has general applicability to studying the interaction of many actin-binding proteins with F-actin, and suggests that caution is needed when comparing different assays for cooperativity within F-actin.

AC proteins use F-actin internal dynamics to disrupt the filament

Because the two ends of an actin filament are different, a potential exists for a steady state, driven by ATP hydrolysis, in which filament length is constant, but protomers are preferentially adding at one end and being removed from the filament at the opposite end (Wegner, 1976). Structurally, one would therefore expect that under such conditions, protomers at the two ends of an actin filament are in different states. Using single particle methods, we have, for the first time, directly visualized two different structural states at the two filament ends. We have recently shown the great advantage of such a single particle approach when dealing with actin-binding proteins that can bind polymorphically and partially decorate F-actin (Galkin et al., 2003).

An obvious question concerns the number of subunits that are in a different conformation at the filament ends. There are two aspects to this question. One involves biochemical differences (having a bound ATP versus ADP), while the other involves structural differences. The two are not simply related, because in the presence of only ADP, one could still have a structural difference between the two ends even though the critical concentration at the two ends must be the same. That is, one end could still be the growing one, and this could be reflected in a structural difference between the two ends. The biochemical differences are potentially simpler to address. One estimate suggested that under steady-state in vitro conditions, there might be ~10 ATP subunits forming a cap (Pieper and Wegner, 1996). An earlier study suggested that the size of the ATP cap would depend upon total actin concentration (Carlier et al., 1985). However, that study also suggested that the interface between ATP-actin and ADP-actin subunits is actually stronger than the interface between two ATP-actin subunits. This could be due to the large degree of cooperativity in F-actin, so that structural changes are propagated through many adjacent subunits. Our own results suggest that the conformational changes at the ends must occur within ~10 subunits. If the changes were in many fewer subunits (one or two), we would not see them, due to averaging. Control experiments (unpublished data) involving segments >20 subunits from the filament ends failed to visualize any conformational changes from the center of the filaments.

Capturing different states at the two ends of an actin filament requires that specimen preparation does not introduce new ends from fragmentation and that there is a reasonable time resolution of the fixation procedure so that subunits are not allowed to change their structural state. We have used a procedure of incubating filaments on the EM grid with F-actin buffer (containing 0.2 mM ATP) after they have been adsorbed to the carbon film so that a steady state might be restored after any filaments were broken. New results have suggested that the process of fixation by staining with uranyl acetate has a time resolution of milliseconds (Zhao and Craig, 2003a,b). We thus expect that the specimen preparation and fixation procedures should preserve the different structural states at the two filament ends. The legitimacy of the assumptions is supported by the fact that we observe two different states.

Under the steady-state conditions that we are using (50 mM KCl, 10 mM Pipes, pH 7.0, 0.2 mM ATP), the barbed end of F-actin is the rapidly growing end. Subunits of G-ATP actin will be adding at this end, and the hydrolysis of ATP to ADP will lag behind the polymerization of these subunits (Carlier et al., 1984). Thus, subunits at this end will be expected to have an ATP bound. The closed nucleotide-binding cleft that we observe in the barbed end reconstruction (Fig. 5 b) is consistent with the observation that this cleft in actin is closed before ATP hydrolysis (Belmont et al., 1999; Sablin et al., 2002). On the other hand, subunits in the center of a filament, as well as at the pointed end, will be expected to have ADP bound, and thus should have an open nucleotide-binding cleft. Consistent with this expectation, we observe such an open conformation for the central segments (Fig. 5 a) as well as for the pointed end (Fig. 5 c).

A more striking difference between the two ends is that the SD1–SD2 contact is substantially disrupted at the pointed, depolymerizing end (Fig. 5 c), but this contact is strong at the barbed, growing end (Fig. 5 b) and in the

center of the filament (Fig. 5 a). The disrupted SD1–SD2 interface seen at the pointed end in pure F-actin is quite similar to the disrupted SD1–SD2 contacts that exist when AC proteins are bound to F-actin (Figs. 1, 2, and 4). It is likely that the disruption of the SD1–SD2 contact will greatly increase the probability that a filament will break at that point (severing), while subunits in this conformation at the ends of filaments will be much more likely to dissociate (depolymerization). Thus, AC proteins bind to F-actin and make the subunits to which they are bound appear similar to the subunits at the depolymerizing end of a pure F-actin filament.

If AC proteins make the subunits in the interior of a filament look like depolymerizing ends, why do AC proteins destabilize the depolymerizing ends and make them depolymerize even faster? An interesting possibility arises from the observation that kinetic rate constants measured during the steady-state phase of F-actin treadmilling (in the absence of other proteins) were 30–45 times higher than the values measured during the initial phase of polymerization (Fujiwara et al., 2002). One explanation for this discrepancy was that during steady state, groups of protomers, rather than single protomers, might be coming off and adding to the filament. Thus, when AC proteins are present at the pointed end, they might allow multiple subunits to be removed from that end, explaining the increase in the observed rate constant for dissociation at that end.

There is a similarity between the disruption of actin's SD1–SD2 interface by AC proteins and the change in F-actin's twist that is induced by AC proteins. We have shown that the twist state in F-actin found when AC proteins bind to F-actin can occur spontaneously in the absence of AC proteins. We suggested that this state is stabilized by the binding of AC proteins, rather than being a novel state induced by these molecules (Galkin et al., 2001). We are now suggesting that the conformation of F-actin, leading to depolymerization and severing, that is induced by the binding of AC proteins is the same conformation that occurs in the absence of AC proteins when a filament is depolymerizing. As we observe no change in the mean twist of naked F-actin at the depolymerizing pointed end (when averaged over ~12 actin protomers), we can separate the change in twist induced by AC proteins from the disruption of the SD1–SD2 interface, which can occur in the absence of a twist change. This is supported by the fact that a set of yeast F-actin segments extensively decorated by y-cofilin was found with a twist of 166.7° (close to the normal twist), and the contact between SD2 and SD1 was completely absent (unpublished data).

A poorly understood feature of actin is the remarkable degree to which its sequence has been conserved over all eukaryotic evolution. For example, there are no amino acid changes between chicken and human skeletal muscle actins, and from yeast to humans, there is ~90% sequence identity of the cytoplasmic actin isoform (Sheterline et al., 1995). One suggestion is that this sequence conservation is due to a remarkable repertoire of internal dynamics and multiple conformational states in F-actin, placing selective pressure on many residues (Egelman, 2001, 2003b). Thus, actin-binding proteins may have evolved to modulate many of these internal modes, rather than to impose new states on the actin filament.

Materials and methods

Specimen preparation and electron microscopy

Complexes of rabbit skeletal muscle actin with pADF were prepared as previously described (Galkin et al., 2001). Wild-type yeast actin, Q41C mutant, and disulfide cross-linked actin were prepared as previously described (Orlova et al., 2001). Y-cofilin was also prepared as previously described (Bobkov et al., 2002), and pADF was a gift from M.-F. Carlier (CNRS, Gif-sur-Yvette, France). Wild-type and Q41C mutant actin were diluted to 3 μM with 50 mM KCl, 10 mM MOPS, pH 7.2, 2 mM $MgCl_2$, 0.5 mM DTT. For disulfide cross-linked actin, the same buffer was used, except DTT was not present. Cofilin was dialyzed against 10 mM MOPS, pH 7.2, with or without 0.5 mM DTT. Actin (3 μM, both wild-type and Q41C mutant) was incubated on glow-discharged carbon-coated EM grids with cofilin (9 μM) for 2 min, followed by negative staining with 2% (wt/vol) uranyl acetate. The disulfide cross-linked actin (3 μM, Q41C mutant) was incubated with y-cofilin (12 μM) for 2 min at room temperature before application to the EM grid and staining. For samples of pure F-actin used in the analysis of filament ends, 7–8 μl of F-actin was applied to the EM grid and allowed to incubate for 2–3 min before staining. A Tecnai-12 electron microscope was used at an accelerating voltage of 80 kV and a nominal magnification of 30,000×. Negatives were densitometered with a Leaf 45 scanner, using a raster of 3.9 Å/pixel.

Image analysis

Complexes of p-ADF with rabbit F-actin. The SPIDER software package (Frank et al., 1996) was used for most of the image processing. Images of pADF complexes with rabbit F-actin (Galkin et al., 2001) were used. The 5,180 images of pADF complexed with rabbit F-actin (pH 6.5) were cross-correlated with the 2,430 projections of the reference models described in the next paragraph. A reconstruction having a mean occupancy by pADF was generated using the iterative helical real space reconstruction (IHRSR) method (Egelman, 2000) from segments selected as having symmetries between 160 and 163°. This set contained 1,205 segments and yielded a stable solution with a twist of 162.2°. To reconstruct segments showing the maximal occupancy by pADF, all images were sorted by the projected density at a radius of 32–48 Å from the helical axis, rather than by the symmetry. The 546 segments (~11%) having the largest density yielded a stable solution at 162.0°. The same symmetry sorting was applied to the complex of pADF with rabbit F-actin (pH 7.7). A subset of 1,311 segments possessing a twist of 161–163° was reconstructed and, after 60 iterations, yielded a stable solution with 162.8°.

Complexes of y-cofilin with wild-type and disulfide cross-linked F-actins. Segments (n = 14,165) of wild-type F-actin decorated with y-cofilin were collected and padded into 100 × 100 pixel boxes. Reconstructions of pure rabbit F-actin at pH 6.5, along with reconstructions of rabbit F-actin singly and doubly occupied by h-ADF at pH 7.7 (Galkin et al., 2001), were used as initial references. New symmetries from 154 to 176°, with a 2° step, were applied to these volumes. Each of these 12 volumes was projected with an azimuthal rotation increment of 4° into 100 × 100 pixel images to yield 3,240 reference projections (12 × 90 × 3), which were cross-correlated with the raw images. After discarding the segments that yielded the highest cross-correlation with pure F-actin and a doubly decorated volume, the remaining segments (having a twist from 160 to 164°) were used to produce a reconstruction of single y-cofilin occupation (n = 1,284, mean twist = 162.2°). This procedure was applied to 14,735 segments of disulfide cross-linked F-actin decorated with y-cofilin. The class of singly occupied segments with a twist of 160–164° contained 3,445 segments and yielded a twist of 162.8°.

Filament ends. Cross-correlation methods against a reference reconstruction were used to determine the polarity of segments cut from filament ends, so that each segment could be classified as being either a "pointed" or "barbed" end. We estimate that ~75% of the segments are assigned with the correct polarity, while ~25% are assigned the wrong polarity. This estimate is based upon both the observed frequency with which the polarity of end segments would reverse during subsequent processing, as well as the statistics for polarity assignment when many segments are cut from the same filament (that must have a uniform polarity). Surprisingly, the overall polarity of the final reconstruction was not improved when filaments having the wrong polarity were removed, due to the fact that these segments are being aligned against a reference having the "correct" polarity. Images of both classes (pointed and barbed) were sorted by symmetry,

and those having a twist of 162–170° were used for the final reconstruction process using the IHRSR method. The barbed end set (n = 321) yielded a symmetry of 166°/27.3 Å, while the pointed end set (n = 422) yielded a symmetry of 166°/27.0 Å.

The significance of the differences between the barbed end and pointed end reconstructions was tested with the following procedure. Initially, a low-pass filtered version of the Holmes model of F-actin (Holmes et al., 1990) was used as a reference for the IHRSR procedure. The segments classified as coming from the barbed end generated one reconstruction, while the segments classified as coming from the pointed end generated a second reconstruction. These reconstructions were then swapped and used as starting references for the segments from the opposite ends of the filament. When the IHRSR procedure started with the pointed end images using the barbed end reconstruction as an initial reference, the resulting reconstruction was almost indistinguishable from the pointed end reconstruction started from the Holmes model. The IHRSR procedure with the barbed end images initiated using the pointed end reconstruction resulted in a reconstruction that was almost indistinguishable from the barbed end reconstruction started from the Holmes model. This established that the differences between these reconstructions were significant and reproducible.

Resolution determination. The widely used Fourier shell correlation (FSC) method of resolution determination (Harauz and van Heel, 1986) is based upon dividing a dataset into two halves, generating reconstructions from each half, and then measuring the correlation of Fourier coefficients between these two reconstructions as a function of resolution. In practice, the two datasets are aligned to a common reference structure, and any noise present can thus become correlated (Grigorieff, 2000; Shaikh et al., 2003; Yang et al., 2003). This measure can yield an unduly optimistic estimate of resolution because the two reconstructions that are being compared are not truly independent. To surmount this, we used the approach (Yang et al., 2003) of starting the IHRSR procedure with the entire dataset from two different initial models, after first demonstrating that these initial models had no significant correlation beyond a very low resolution (~35 Å). After convergence of the IHRSR procedure from these two different starting points, the two resulting reconstructions are compared. Using the conservative standard of FSC = 0.5 as the resolution limit, the poorest dataset (due to a limited number of segments), involving the filament ends from naked F-actin, yielded a resolution of ~23 Å. All other datasets were comparable or better in resolution.

Atomic models. Manual fitting of atomic structures for the actin monomer (PDB entry 2BTF) and plant ADF-1 from *Arabidopsis thaliana* (PDB entry 1F76) were done using the crystallographic package O (Jones et al., 1991). A 3D surface of each atomic structure was generated using a comparable resolution (20 Å) to that of the actin–AC reconstructions. The crystallographic surfaces were docked into the reconstructions using shape as the primary guide. For actin, the fit of the crystal structure was unambiguous; however, there were multiple orientations of the AC structures that produced reasonable fits to the 3D reconstructions. In the models for the disulfide actin, we engineered a Gln41Cys mutant, imposed a S–S crosslink, and ran mild energy minimization to relieve sterical strain on the new disulfide using SYBYL (Tripos, Inc.).

This work was supported by National Institutes of Health (NIH) AR424023 and EB001567 (to E.H. Egelman) and NIH AR22031 and National Science Foundation MCB9904599 (to E. Reisler).

Submitted: 27 August 2003
Accepted: 20 October 2003

References

Abe, H., T. Obinata, L.S. Minamide, and J.R. Bamburg. 1996. *Xenopus laevis* actin-depolymerizing factor/cofilin: a phosphorylation-regulated protein essential for development. *J. Cell Biol.* 132:871–885.

Bamburg, J.R. 1999. Proteins of the ADF/cofilin family: essential regulators of actin dynamics. *Annu. Rev. Cell Dev. Biol.* 15:185–230.

Belmont, L.D., A. Orlova, D.G. Drubin, and E.H. Egelman. 1999. A change in actin conformation associated with filament instability after Pi release. *Proc. Nat. Acad. Sci. USA.* 96:29–34.

Blondin, L., V. Sapountzi, S.K. Maciver, C. Renoult, Y. Benyamin, and C. Roustan. 2001. The second ADF/cofilin actin-binding site exists in F-actin, the cofilin-G-actin complex, but not in G-actin. *Eur. J. Biochem.* 268:6426–6434.

Bobkov, A.A., A. Muhlrad, K. Kokabi, S. Vorobiev, S.C. Almo, and E. Reisler. 2002. Structural effects of cofilin on longitudinal contacts in F-actin. *J. Mol. Biol.* 323:739–750.

Bowman, G.D., I.M. Nodelman, Y. Hong, N.H. Chua, U. Lindberg, and C.E. Schutt. 2000. A comparative structural analysis of the ADF/cofilin family. *Proteins.* 41:374–384.

Bremer, A., C. Henn, K.N. Goldie, A. Engel, P.R. Smith, and U. Aebi. 1994. Towards atomic interpretation of F-actin filament three-dimensional reconstructions. *J. Mol. Biol.* 242:683–700.

Carlier, M.F. 1998. Control of actin dynamics. *Curr. Opin. Cell Biol.* 10:45–51.

Carlier, M.F., and D. Pantaloni. 1997. Control of actin dynamics in cell motility. *J. Mol. Biol.* 269:459–467.

Carlier, M.F., D. Pantaloni, and E.D. Korn. 1984. Evidence for an ATP cap at the ends of actin filaments and its regulation of the F-actin steady state. *J. Biol. Chem.* 259:9983–9986.

Carlier, M.F., V. Laurent, J. Santolini, R. Melki, D. Didry, G.X. Xia, Y. Hong, N.H. Chua, and D. Pantaloni. 1997. Actin depolymerizing factor (ADF/cofilin) enhances the rate of filament turnover: implication in actin-based motility. *J. Cell Biol.* 136:1307–1322.

Carlier, M.F., D. Pantaloni, and E.D. Korn. 1985. Polymerization of ADP-actin and ATP-actin under sonication and characteristics of the ATP-actin equilibrium polymer. *J. Biol. Chem.* 260:6565–6571.

Chik, J.K., U. Lindberg, and C.E. Schutt. 1996. The structure of an open state of β-actin at 2.65 Ångstrom resolution. *J. Mol. Biol.* 263:607–623.

Coluccio, L.M., and L.G. Tilney. 1983. Under physiological conditions actin disassembles slowly from the nonpreferred end of an actin filament. *J. Cell Biol.* 97:1629–1634.

Combeau, C., and M.F. Carlier. 1988. Probing the mechanism of ATP hydrolysis on F-actin using vanadate and the structural analogs of phosphate BeF-3 and A1F-4. *J. Biol. Chem.* 263:17429–17436.

Cooper, J.A., J.D. Blum, R.C. Williams, Jr., and T.D. Pollard. 1986. Purification and characterization of actophorin, a new 15,000-dalton actin-binding protein from *Acanthamoeba castellanii*. *J. Biol. Chem.* 261:477–485.

Dedova, I.V., V.N. Dedov, N.J. Nosworthy, B.D. Hambly, and C.G. dos Remedios. 2002. Cofilin and DNase I affect the conformation of the small domain of actin. *Biophys. J.* 82:3134–3143.

Egelman, E.H. 2000. A robust algorithm for the reconstruction of helical filaments using single-particle methods. *Ultramicroscopy.* 85:225–234.

Egelman, E.H. 2001. Molecular evolution: actin's long lost relative found. *Curr. Biol.* 11:R1022–R1024.

Egelman, E.H. 2003a. A tale of two polymers: new insights into helical filaments. *Nat. Rev. Mol. Cell Biol.* 4:621–630.

Egelman, E.H. 2003b. Actin's prokaryotic homologs. *Curr. Opin. Struct. Biol.* 13: 244–248.

Frank, J., M. Radermacher, P. Penczek, J. Zhu, Y. Li, M. Ladjadj, and A. Leith. 1996. SPIDER and WEB: processing and visualization of images in 3D electron microscopy and related fields. *J. Struct. Biol.* 116:190–199.

Fujiwara, I., S. Takahashi, H. Tadakuma, T. Funatsu, and S. Ishiwata. 2002. Microscopic analysis of polymerization dynamics with individual actin filaments. *Nat. Cell Biol.* 4:666–673.

Galkin, V.E., A. Orlova, N. Lukoyanova, W. Wriggers, and E.H. Egelman. 2001. Actin depolymerizing factor stabilizes an existing state of F-actin and can change the tilt of F-actin subunits. *J. Cell Biol.* 153:75–86.

Galkin, V.E., M.S. VanLoock, A. Orlova, and E.H. Egelman. 2002. A new internal mode in F-actin helps explain the remarkable evolutionary conservation of actin's sequence and structure. *Curr. Biol.* 12:570–575.

Galkin, V.E., A. Orlova, M.S. VanLoock, and E.H. Egelman. 2003. Do the utrophin tandem calponin homology domains bind F-actin in a compact or extended conformation? *J. Mol. Biol.* 331:967–972.

Grigorieff, N. 2000. Resolution measurement in structures derived from single particles. *Acta Crystallogr. D Biol. Crystallogr.* 56:1270–1277.

Harauz, G., and M.G. van Heel. 1986. Exact filters for general geometry three-dimensional reconstruction. *Optik*. 73:146–156.

Holmes, K.C., D. Popp, W. Gebhard, and W. Kabsch. 1990. Atomic model of the actin filament. *Nature.* 347:44–49.

Jones, T.A., J.Y. Zou, S.W. Cowan, and M. Kjeldgaard. 1991. Improved methods for binding protein models in electron density maps and the location of errors in these models. *Acta Crystallogr. A.* 47:110–119.

Kim, E., W. Wriggers, M. Phillips, K. Kokabi, P.A. Rubenstein, and E. Reisler. 2000. Cross-linking constraints on F-actin structure. *J. Mol. Biol.* 299: 421–429.

Lappalainen, P., and D.G. Drubin. 1997. Cofilin promotes rapid actin filament turnover in vivo. *Nature.* 388:78–82.

Maciver, S.K., and A.G. Weeds. 1994. Actophorin preferentially binds monomeric ADP-actin over ATP-bound actin: consequences for cell locomotion. *FEBS Lett.* 347:251–256.

Maciver, S.K., H.G. Zot, and T.D. Pollard. 1991. Characterization of actin filament severing by actophorin from *Acanthamoeba castellanii*. *J. Cell Biol.* 115: 1611–1620.

Maciver, S.K., B.J. Pope, S. Whytock, and A.G. Weeds. 1998. The effect of two actin depolymerizing factors (ADF/cofilins) on actin filament turnover: pH sensitivity of F-actin binding by human ADF, but not of *Acanthamoeba* actophorin. *Eur. J. Biochem.* 256:388–397.

McGough, A., and W. Chiu. 1999. ADF/cofilin weakens lateral contacts in the actin filament. *J. Mol. Biol.* 291:513–519.

McGough, A., B. Pope, W. Chiu, and A. Weeds. 1997. Cofilin changes the twist of F-actin: implications for actin filament dynamics and cellular function. *J. Cell Biol.* 138:771–781.

McLaughlin, P.J., J.T. Gooch, H.G. Mannherz, and A.G. Weeds. 1993. Structure of gelsolin segment 1-actin complex and the mechanism of filament severing. *Nature.* 364:685–692.

Ono, S., A. McGough, B.J. Pope, V.T. Tolbert, A. Bui, J. Pohl, G.M. Benian, K.M. Gernert, and A.G. Weeds. 2001. The C-terminal tail of UNC-60B (actin depolymerizing factor/cofilin) is critical for maintaining its stable association with F-actin and is implicated in the second actin-binding site. *J. Biol. Chem.* 276:5952–5958.

Orlova, A., and E.H. Egelman. 1993. A conformational change in the actin subunit can change the flexibility of the actin filament. *J. Mol. Biol.* 232:334–341.

Orlova, A., and E.H. Egelman. 1995. Structural dynamics of F-actin. I. Changes in the C-terminus. *J. Mol. Biol.* 245:582–597.

Orlova, A., E. Prochniewicz, and E.H. Egelman. 1995. Structural dynamics of F-actin. II. Co-operativity in structural transitions. *J. Mol. Biol.* 245:598–607.

Orlova, A., V.E. Galkin, M.S. VanLoock, E. Kim, A. Shvetsov, E. Reisler, and E.H. Egelman. 2001. Probing the structure of f-actin: cross-links constrain atomic models and modify actin dynamics. *J. Mol. Biol.* 312:95–106.

Otterbein, L.R., P. Graceffa, and R. Dominguez. 2001. The crystal structure of uncomplexed actin in the ADP state. *Science.* 293:708–711.

Owen, C., and D. DeRosier. 1993. A 13 A map of the actin-scruin filament from the limulus acrosomal process. *J. Cell Biol.* 123:337–344.

Pieper, U., and A. Wegner. 1996. The end of a polymerizing actin filament contains numerous ATP-subunit segments that are disconnected by ADP-subunits resulting from ATP hydrolysis. *Biochemistry.* 35:4396–4402.

Pope, B.J., S.M. Gonsior, S. Yeoh, A. McGough, and A.G. Weeds. 2000. Uncoupling actin filament fragmentation by cofilin from increased subunit turnover. *J. Mol. Biol.* 298:649–661.

Ressad, F., D. Didry, G.X. Xia, Y. Hong, N.H. Chua, D. Pantaloni, and M.F. Carlier. 1998. Kinetic analysis of the interaction of actin-depolymerizing factor (ADF)/cofilin with G- and F-actins. Comparison of plant and human ADFs and effect of phosphorylation. *J. Biol. Chem.* 273:20894–20902.

Sablin, E.P., J.F. Dawson, M.S. VanLoock, J.A. Spudich, E.H. Egelman, and R.J. Fletterick. 2002. How does ATP hydrolysis control actin's associations? *Proc. Natl. Acad. Sci. USA.* 99:10945–10947.

Sampath, P., and T.D. Pollard. 1991. Effects of cytochalasin, phalloidin, and pH on the elongation of actin filaments. *Biochemistry.* 30:1973–1980.

Schutt, C.E., J.C. Myslik, M.D. Rozycki, N.C.W. Goonesekere, and U. Lindberg. 1993. The structure of crystalline profilin:β-actin. *Nature.* 365:810–816.

Shaikh, T.R., R. Hegerl, and J. Frank. 2003. An approach to examining model dependence in EM reconstructions using cross-validation. *J. Struct. Biol.* 142: 301–310.

Sheterline, P., J. Clayton, and J. Sparrow. 1995. Actin. *Protein Profile.* 2:1–103.

Wegner, A. 1976. Head to tail polymerization of actin. *J. Mol. Biol.* 108:139–150.

Yang, S., X. Yu, V.E. Galkin, and E.H. Egelman. 2003. Issues of resolution and polymorphism in single-particle reconstruction. *J. Struct. Biol.* In press.

Yeoh, S., B. Pope, H.G. Mannherz, and A. Weeds. 2002. Determining the differences in actin binding by human ADF and cofilin. *J. Mol. Biol.* 315:911–925.

Yonezawa, N., E. Nishida, and H. Sakai. 1985. pH control of actin polymerization by cofilin. *J. Biol. Chem.* 260:14410–14412.

Zhao, F.Q., and R. Craig. 2003a. Ca^{2+} causes release of myosin heads from the thick filament surface on the milliseconds time scale. *J. Mol. Biol.* 327:145–158.

Zhao, F.Q., and R. Craig. 2003b. Capturing time-resolved changes in molecular structure by negative staining. *J. Struct. Biol.* 141:43–52.